Editors' Suggestion

Anchoring Effect of an Obstacle in the Silo Unclogging Process

Rodrigo Caitano, Angel Garcimartín,* and Iker Zuriguel
Departamento de Física, Facultad de Ciencias, Universidad de Navarra, E-31080 Pamplona, Spain

(Received 3 February 2023; accepted 20 July 2023; published 31 August 2023)

Contrary to the proven beneficial role that placing an obstacle above a silo exit has in clogging prevention, we demonstrate that, when the system is gently shaken, this passive element has a twofold effect in the clogging destruction process. On one side, the obstacle eases the destruction of weak arches, a phenomenon that can be explained by the pressure screening that it causes in the outlet proximities. But on the other side, we discover that the obstacle presence leads to the development of a few very strong arches. These arches, which dominate in the heavy tailed distributions of unclogging times, correlate with configurations where the number of particles contacting the obstacle from below are higher than the average; hence suggesting that the obstacle acts as an anchoring point for the granular packing. This finding may help one to understand the ambiguous effect of obstacles in the bottleneck flow of other systems, such as pedestrians evacuating a room or active matter in general.

DOI: 10.1103/PhysRevLett.131.098201

The suitable placement of an obstacle in front of a bottleneck is known to be beneficial in terms of flow enhancement for particulated materials. This strategy, originally implemented for the discharge of granular materials from silos [1,2] was afterward generalized to other systems, such as pedestrian flows [3] and animal streams [4]. Curiously, the use of obstacles in pedestrian evacuations is the scenario arising the most interest, yet controversy still goes on about the efficiency of this procedure [5]. Thus, in a recent work it was suggested that, in highly competitive conditions, the effect of the obstacle on the flow rate is negligible [6]. On the contrary, there is an agreement about the positive effect of an obstacle suitably placed above the exit of a silo in terms of clogging reduction and granular outflow [7–11]. Indeed, it is accepted that the obstacle may lead to a decrease of the probability of clogging by more than 2 orders of magnitude, while keeping the flow rate almost unaltered (maximum 10%). But even in the silo case, there are some exceptions such as the one revealed by Wang *et al.*, who demonstrated that the obstacle effect is negligible when the granular material is conformed by soft spheres [12]. And yet this exception fails for an extreme case of deformable particles (droplets) flowing through constrictions, adding further confusion. In this scenario, in which the droplet breakage is tantamount to the clogging process of rigid grains, it has been experimentally proved that the obstacle presence reduces breaking probability by almost 3 orders of magnitude [13].

At the core of this conundrum is the fact that discrete systems flowing through constrictions display intermittent dynamics, with flowing intervals interspersed by clogging ones [4,14–16]. This behavior occurs when blocking structures develop and then shatter if they are not able to resist a given energy input. The source of this energy can be intrinsic to the agents (like in the case of animals, humans, or active particles, in general), externally imposed (in a vibrated silo), or arise from an energy unbalance within the system (storage and release of elastic energy in the case of soft particles). Anyway, the flow in the intermittent regime is determined by two processes: (1) the probability of clog formation, which defines the duration of "flowing intervals" (t_f) and (2) the probability of clog destruction, which sets the duration of "clogged intervals" (t_c). Importantly, clogging and unclogging processes are well differentiated as they display distinctive statistical features. Then, it should not come as a surprise that the obstacle effect on them is not equally important. Even more, it should not be discarded that the obstacle could affect both processes in different manners in terms of global flow improvement. But as far as we know, there is not any investigation about the way in which an obstacle placed upstream a bottleneck affects the unclogging process in an independent manner from the clogging one. This is indeed the goal of this Letter, where we make use of the simplest possible system, i.e., hard inert grains flowing out of a silo that is externally vibrated. In this way, we discover that the presence of the obstacle (which always prevents clog formation) may lead to either (i) an acceleration of the clog destruction process (flow rate improvement) and (ii) the development of a few very strong arches that cause an overall flow rate reduction.

The experimental setup is the same described in [17]. It consists of a thin silo (300 mm wide, 800 mm high, and 1.20 ± 0.05 mm thick) containing a monolayer of stainless steel monodisperse spheres (diameter 1.00 ± 0.01 mm). The orifice at the base is made with two movable flanges separated among them [Fig. 1(a)], hence conforming an outlet of size $d = 2.83 \pm 0.05$ mm. The flanges are

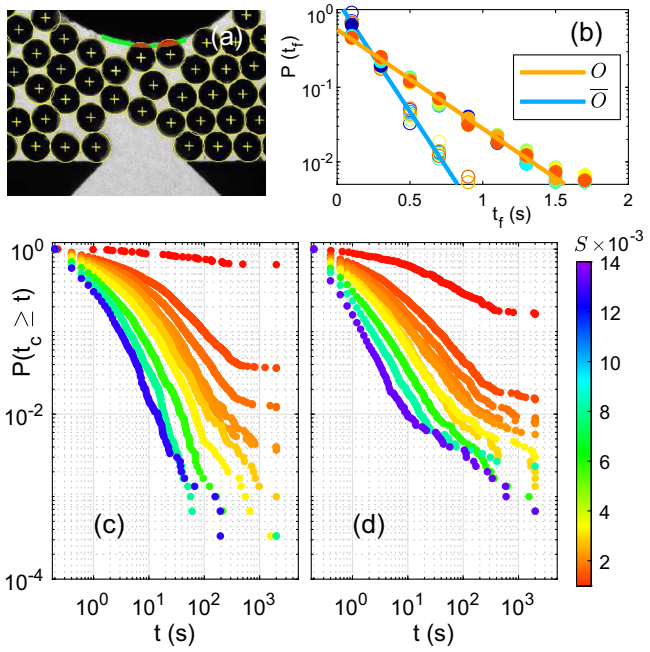

FIG. 1. (a) Photograph of the outlet; the lowest part of the obstacle can be observed. Beads are marked with yellow circles and their centers with yellow crosses. Contacts among beads and the obstacle just above the orifice (green line) are marked in red. (b) Exponential distributions (note the log-lin scale) of the flowing time intervals (t_f) for the cases with (O, filled symbols) and without ($\bar{O}$, empty symbols) an obstacle above the orifice. The corresponding characteristic times are $\tau = 0.33$ and $\tau = 0.15$ s. The survival functions of the clogging times are displayed in (c) for a silo without an obstacle and in (d) for the silo with an obstacle, both in log-log scale. Colors (see color bar) encode the value of S.

isolated from the rest of the silo, so they can oscillate vertically while the rest of the silo remains static. The vibration, of amplitude A and frequency $\omega = 2\pi f$ (with $f = 90$ Hz; other values are reported in the Supplemental Material [18]), is characterized by $S = A\omega/\sqrt{gl}$, where g is the gravity acceleration, and l is a characteristic length for which we use the bead diameter. Note that S is a nondimensional velocity that can be interpreted as the square root of the ratio between kinetic and potential energy [21,22] and was already shown to be a good control parameter in the description of silo unclogging as a continuous transition [17]. As a novelty, in this Letter, we place a static obstacle above the orifice. The obstacle is a disk of diameter 8.90 ± 0.05 mm with its lowest point at $h = 3.95 \pm 0.05$ mm above the orifice and vertically aligned with it [see Fig. 1(a)]. This value of h (two others are reported in the Supplemental Material [18]) was chosen because it is close to the position where clog formation is reduced the most [7]. Also, at this position most of the arches span across the orifice (less than one in 10 000 block the exit by forming instead two lateral arches spanning from the silo base to the obstacle).

The procedure implemented here differs from previous studies in that the silo is only vibrated when a clog develops; i.e., the silo is stopped while the system is flowing. This protocol was conceived to univocally separate the flowing and clogging intervals. Then, the silo (with the base at rest) was filled and the grains started to pass through the outlet. When an arch blocked the orifice (an instance that was detected when the flow was interrupted during 5 s), the end of the flowing interval t_f was determined at the moment of the passage of the last particle. After that, the vibration was applied until a bead crossed the outlet, marking the end of the clogging time interval (t_c). This event also flags the beginning of a new flowing interval. Then, the procedure was repeated as many times as wanted, typically more than 3000. Note that in the hypothetical case a clogging arch was not shattered after 2000 s, a stronger vibration was applied, and the clogging time registered as "censored" (longer than 2000 s). The resolution of all temporal measurements was conditioned by the frame acquisition rate (100 frames/s); but this being smaller than the typical time it takes for one bead passing through the outlet, we decided to assign a minimum of 0.2 s to both t_f and t_c.

We start by representing the distributions of both flowing and clogging intervals for all the vibration strengths implemented, with and without an obstacle above the orifice. The flowing intervals (or avalanche durations) represented in Fig. 1(b) evidence exponential decays in all the cases, corroborating the known result that the clogging probability remains constant during the whole avalanche duration [23–26]. As expected, the distributions of flowing times are independent of S (recall that the vibration was off when the system was flowing). On the contrary, there is an important effect of the obstacle on the avalanche duration. Indeed, the characteristic time (see caption) is more than doubled when the obstacle is present, which is an important reduction of the probability of clogging. All these features just confirm previous results about clogging prevention by obstacles in static silos [7].

The analysis of clogging times [Figs. 1(c) and 1(d)] reveals completely different distributions, with tails broader than exponential (note the logarithmic scale). This implies an arch breaking probability that is not constant over time (it decreases as time goes by), a behavior whose physical origin is still under active debate [27,28]. In order to better visualize the distribution tails, it is convenient to compute the survival distributions, a representation that is well suited for the censored data of this experiment (note that, for some clogging times, we only know they are longer than 2000 s). A first inspection of Figs. 1(c) and 1(d) evidences that, no matter if the obstacle is present or not, increasing S leads to a downward displacement of the curves; hence the probability of finding long clogs is reduced. More importantly, a close comparison of both plots reveals an intriguing feature: in the presence of the obstacle [Fig. 1(d)], the

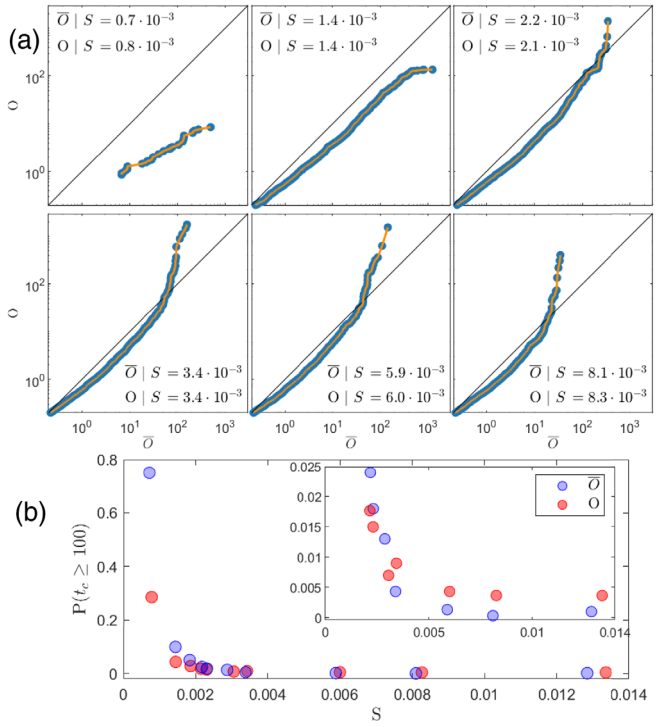

FIG. 2. (a) Q-Q plots of the clogging time distributions for the silo with obstacle O against the silo without obstacle $\bar{O}$. The values of S, which have been chosen to be as similar as possible, are indicated in each panel. The continuous black line indicates $O = \bar{O}$, so points below (above) this line indicate a scenario in which the presence of the obstacle reduces (increases) clogging times. (b) Probability of finding a clogging time longer than 100 s vs the vibration strength S for the cases with and without obstacle (see legend). Inset: an enlargement of $P(t_c \geq 100) < 0.025$.

tails corresponding to different values of S are less scattered than in the no-obstacle case [Fig. 1(c)]. And this is the result of both (1) a downward displacement of the curve obtained for the smallest S with obstacle with respect to the corresponding one without the obstacle [red in Figs. 1(c) and 1(d), corresponding to $S \simeq 0.7 \times 10^{-3}$] and (2) an upward displacement of the curve obtained for the largest S with obstacle with respect to the corresponding one without the obstacle [blue in Figs. 1(c) and 1(d)]. If confirmed, this would imply a counterintuitive effect: the obstacle reduces the amount of long clogs when S is small, but favors their development when S is large.

In order to better compare the scenarios with (O) and without ($\bar{O}$) obstacle, we have computed the Q-Q plots of their respective clogging time distributions for similar vibration strength [Fig. 2(a)]. In the x axis, the condition $\bar{O}$ is represented as a reference. For the two lowest values of S displayed, all data appear below the line $O = \bar{O}$, proving the beneficial role of the obstacle in terms of reducing the clogging times. Nevertheless, for vibration strengths above $S \approx 2.0 \times 10^{-3}$, a crossover becomes patent. This crossover implies that the obstacle induces a reduction of the duration of short clogs, but an increase of the long ones. Indeed, as S increases, it seems obvious that the crossover occurs for lower clogging times, going from about 200 s when $S \approx 2.1 \times 10^{-3}$ to 20 s when $S \approx 8.1 \times 10^{-3}$. In summary, from the Q-Q plots we evidence that the obstacle always reduces the duration of the short clogs (no matter the value of S), whereas it reduces or enlarges the duration of the longest clogs depending on the vibration strength. The discovery of this behavior is relevant as it constitutes the first evidence of the obstacle reducing the flow rate in a vibrated silo, in a scenario in which it is clearly beneficial in terms of clog prevention (in both, a static silo and a vibrated one). Aiming to confirm this latter behavior, in Fig. 2(b) we represent the probability of finding clogs longer than 100 s (we take this number as an example of what we consider long clogs) vs S, for the obstacle and no-obstacle scenarios. The plot shows that, for low values of S, the data points for the silo without obstacle are above the ones for the silo with an obstacle, hence demonstrating the beneficial role of the obstacle in terms of reducing clogging times. However, a magnification of the low values of P (inset) allows appreciation of a crossover from a region where the obstacle facilitates breaking of long-standing arches (low values of S) to another one in which these long-standing arches become more robust in the presence of the obstacle (high values of S).

After confirming that the obstacle reduces duration of short clogs but has a dual effect on long clogs (reducing their amount when S is small and increasing it when S is large), we investigated the physical reasons behind this unexpected behavior. To this end, we resorted to analyzing the grain arrangements above the clogging arches; in particular, we focused on the configurations in which grains were touching the lowest part of the obstacle. We thought that these configurations, in which the obstacle could act as a support point for beads below it, were good candidates to be behind the increase of long clog durations. Therefore, for each clog, we tried to estimate the anchoring level by computing the number of beads n_c touching the lowest part of the obstacle in the region just above the orifice as represented in Fig. 1(a) (this configuration, for instance, corresponds to $n_c = 2$). After this, in Fig. 3 we represented the survival functions of the clogging times for different values of S, but discriminated configurations depending on the value of n_c. Interestingly, all distributions are almost identical when S is low [Fig. 3(a)] indicating a negligible role of the anchoring. In this scenario, only very weak arches are destroyed, and it is well known that these ones are primarily conditioned by the arch structure [29] and the weight above them [4]. Accordingly, the pressure reduction that the obstacle introduces leads to a decrease of the clog duration which is independent of n_c (note the lower values of all curves for different n_c with respect to the case without obstacle). Interestingly, the differences among the curves corresponding to structures with different n_c

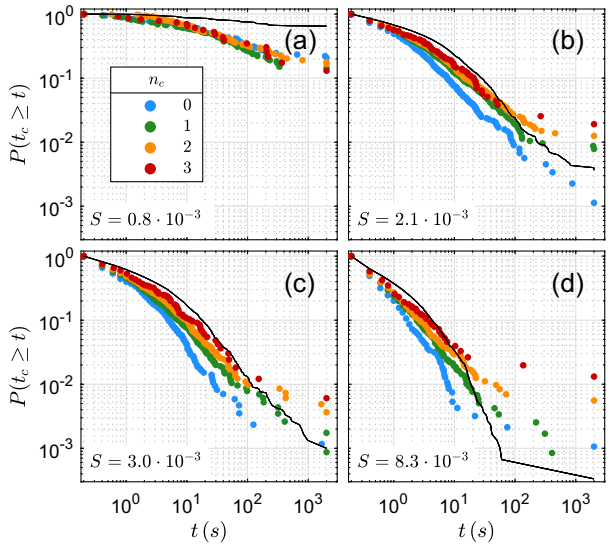

FIG. 3. Survival functions of t_c when grouping the data depending on n_c, the number of grains contacting the lowest part of the obstacle (see legend). Black lines correspond to the survival functions obtained for the case without an obstacle. Figures (a–d) show results obtained for increasing values of S as indicated in the bottom-left corner.

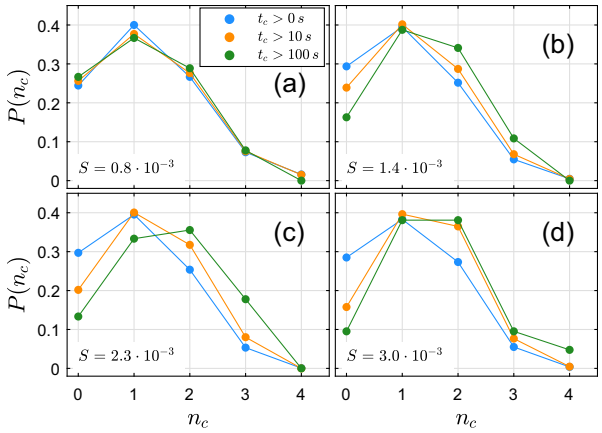

FIG. 4. Probability that a configuration has n_c particles contacting the obstacle in the region marked with a green line in Fig. 1. Distinct colors are used for different groups of configurations depending on the time they have resisted before collapsing [see legend (a)]. Figures (a–d) show the distributions obtained for increasing values of S as indicated in the bottom-left corner.

become clear when S grows [Figs. 3(b)–3(d)], especially for long clogging times. Two features should be highlighted there: (i) The higher n_c is, the greater the probability of finding long clogging times; i.e., the stronger the anchoring, the longer the arches resist the vibration. (ii) The distributions obtained for $n_c = 0$ fall systematically below the curves obtained for the case without an obstacle (black lines), whereas the ones for $n_c > 1$ fall above. This behavior definitively proves the dual role of the obstacle in relation to clog destruction. On one side, the obstacle reduces pressure at the orifice facilitating arch breaking (this is visible for $n_c = 0$ when anchoring is minimized); on the other, the obstacle allows the anchoring of the structure, hence providing extra resistance to the arches (this is clearly visible for $n_c = 2$ or 3).

An alternative way of proving the importance of anchoring among the obstacle and the outlet in the development of long clogging times when the vibration strength is high is representing the distribution of configurations according to n_c. This is done in Fig. 4 for different values of S (in each panel) and grouping the data depending on the t_c associated with each granular configuration. Note that the distributions for $t_c > 0$ are necessarily similar in all panels as correspond to all arches formed before applying the vibration. Compared with these, we observe no differences in the distributions for the smallest value of S [Fig. 4(a)], corroborating that in this scenario anchoring does not affect the arch stability. On the contrary, when S grows [Figs. 4(b)–4(d)] there is a shift in the distributions toward higher values of n_c as the associated clogging times enlarge. Indeed, when $S > 2 \times 10^{-3}$ [Figs. 4(c) and 4(d)] the proportion of scenarios with $n_c > 1$ is about 30% if we consider all configurations, but grows above 50% for $t_c > 100$ s. This confirms that the most resistant clogs are associated with configurations where the number of particles contacting the obstacle from below is more abundant than the average, hence supporting the hypothesis of the obstacle acting as an anchoring point.

In summary, we have carried out a thorough analysis of the flowing and clogging intervals of granular bottleneck flow combined with the characterization of the packing configuration above the arch developed for each clog. Although in this Letter results are presented only for a given obstacle position and vibration frequency ω, we have tested the robustness of our findings against the variation of these parameters (see Supplemental Material [18]). All this has allowed us to discover a novel role of the obstacle, which can act as an anchoring point for some (very few) structures, hence leading to very long clogging times. This negative effect of the obstacle (which is marginally compensated by a positive one in terms of reducing the duration of short clogs) is only visible when the magnitude of the vibration strength is high. On the contrary, when the vibration strength is low, the obstacle has only a positive effect, reducing both the duration of short and long clogs. Our hypothesis is that, when S is low, the dynamics are very slow and only very weak arches break, so the pressure reduction at the outlet region imposed by the obstacle dominates the process favoring unclogging. On the contrary, for high vibration strengths (where 99% of the arches quickly break in less than 10 s) the presence of the obstacle can serve as an anchoring point, hence preventing unclogging. It is meaningful that many experiments in other systems (such as pedestrian flows) are also characterized by fast dynamics, so the ambiguous results reported in the

literature may be explained by the anchoring effect of the obstacle.

We thank L. F. Urrea for technical help. This work was funded by Ministerio de Economía y Competitividad (Spanish Government) through Project No. PID2020–114839 GB-I00 MINECO/AEI/FEDER, UE. R. C. acknowledges Asociación de Amigos de la Universidad de Navarra for his grant.

*angel@unav.es

[1] A. W. Jenike, Storage and flow of solids, Bulletin No. 123, Utah Engineering Experimental Station, University of Utah, 1964, https://digital.library.unt.edu/ark:/67531/metadc1067072/.

[2] U. Tüzün and R. M. Nedderman, Gravity flow of granular materials round obstacles—I: Investigation of the effects of inserts on flow patterns inside a silo, Chem. Eng. Sci. **40**, 325 (1985).

[3] D. Helbing, I. J. Farkas, and T. Vicsek, Simulating dynamical features of escape panic, Nature (London) **407**, 487 (2000).

[4] I. Zuriguel, D. R. Parisi, R. C. Hidalgo, C. Lozano, A. Janda, P. A. Gago, J. P. Peralta, L. M. Ferrer, L. A. Pugnaloni, E. Clément, D. Maza, I. Pagonabarraga, and A. Garcimartín, Clogging transition of many-particle systems flowing through bottlenecks, Sci. Rep. **4**, 7324 (2014).

[5] N. Shiwakoti, X. Shi, and Z. Ye, A review on the performance of an obstacle near an exit on pedestrian crowd evacuation, Saf. Sci. **113**, 54 (2019).

[6] A. Garcimartín, D. Maza, J. M. Pastor, D. R. Parisi, C. Martín-Gómez, and I. Zuriguel, Redefining the role of obstacles in pedestrian evacuation, New J. Phys. **20**, 123025 (2018).

[7] I. Zuriguel, A. Janda, A. Garcimartín, C. Lozano, R. Arévalo, and D. Maza, Silo Clogging Reduction by the Presence of an Obstacle, Phys. Rev. Lett. **107**, 278001 (2011).

[8] K. Endo, K. A. Reddy, and H. Katsuragi, Obstacle-shape effect in a two-dimensional granular silo flow field, Phys. Rev. Fluids **2**, 094302 (2017).

[9] A. V. K. Reddy, S. Kumar, K. A. Reddy, and J. Talbot, Granular silo flow of inelastic dumbbells: Clogging and its reduction, Phys. Rev. E **98**, 022904 (2018).

[10] A. B. Harada, E. Thackray, and K. N. Nordstrom, Silo flow and clogging in the presence of an obstacle, Phys. Rev. Fluids **7**, 054301 (2022).

[11] D. Gella, D. Yanagisawa, R. Caitano, M. V. Ferreyra, and I. Zuriguel, On the dual effect of obstacles in preventing silo clogging in 2D, Commun. Phys. **5**, 4 (2022).

[12] J. Wang, K. Harth, D. Puzyrev, and R. Stannarius, The effect of obstacles near a silo outlet on the discharge of soft spheres, New J. Phys. **24**, 093010 (2022).

[13] A. D. Bick, J. W. Khor, Y. Gai, and S. K. Y. Tang, Strategic placement of an obstacle suppresses droplet break up in the hopper flow of a microfluidic soft crystal, Proc. Natl. Acad. Sci. U.S.A. **118**, e2017822118 (2021).

[14] D. Helbing, A. Johansson, J. Mathiesen, M. H. Jensen, and A. Hansen, Analytical Approach to Continuous and Intermittent Bottleneck Flows, Phys. Rev. Lett. **97**, 168001 (2006).

[15] M. Souzy, I. Zuriguel, and A. Marin, Transition from clogging to continuous flow in constricted particle suspensions, Phys. Rev. E **101**, 060901(R) (2020).

[16] T. Knippenberg, A. Lüders, C. Lozano, P. Nielaba, and C. Bechinger, Role of cohesion in the flow of active particles through bottlenecks, Sci. Rep. **12**, 11525 (2022).

[17] R. Caitano, B. V. Guerrero, R. E. R. González, I. Zuriguel, and A. Garcimartín, Characterization of the Clogging Transition in Vibrated Granular Media, Phys. Rev. Lett. **127**, 148002 (2021).

[18] See Supplemental Material at http://link.aps.org/supplemental/10.1103/PhysRevLett.131.098201 for a discussion of the vibration characterization and a generalization of our results to another outlet size, which includes Refs. [17,19,20].

[19] C. Lozano, A. Janda, A. Garcimartín, D. Maza, and I. Zuriguel, Flow and clogging in a silo with an obstacle above the orifice, Phys. Rev. E **86**, 031306 (2012).

[20] A. Pascot, N. Gaudel, S. Antonyuk, J. Bianchin, and S. Kiesgen de Richter, Influence of mechanical vibrations on quasi-2D silo discharge of spherical particles, Chem. Eng. Sci. **224**, 115749 (2020).

[21] C. R. Wassgren, M. L. Hunt, P. J. Freese, J. Palamara, and C. E. Brennen, Effects of vertical vibration on hopper flows of granular material, Phys. Fluids **14**, 3439 (2002).

[22] P. Eshuis, K. Van Der Weele, D. Van Der Meer, R. Bos, and D. Lohse, Phase diagram of vertically shaken granular matter, Phys. Fluids **19**, 123301 (2007).

[23] I. Zuriguel, L. A. Pugnaloni, A. Garcimartín, and D. Maza, Jamming during the discharge of grains from a silo described as a percolating transition, Phys. Rev. E **68**, 030301(R) (2003).

[24] T. Masuda, K. Nishinari, and A. Schadschneider, Critical Bottleneck Size for Jamless Particle Flows in Two Dimensions, Phys. Rev. Lett. **112**, 138701 (2014).

[25] K. To, Jamming transition in two-dimensional hoppers and silos, Phys. Rev. E **71**, 060301(R) (2005).

[26] C. C. Thomas and D. J. Durian, Geometry dependence of the clogging transition in tilted hoppers, Phys. Rev. E **87**, 052201 (2013).

[27] C. Merrigan, S. K. Birwa, S. Tewari, and B. Chakraborty, Ergodicity breaking dynamics of arch collapse, Phys. Rev. E **97**, 040901(R) (2018).

[28] A. Nicolas, A. Garcimartín, and I. Zuriguel, Trap Model for Clogging and Unclogging in Granular Hopper Flows, Phys. Rev. Lett. **120**, 198002 (2018).

[29] C. Lozano, G. Lumay, I. Zuriguel, R. C. Hidalgo, and A. Garcimartín, Breaking Arches with Vibrations: The Role of Defects, Phys. Rev. Lett. **109**, 068001 (2012).